

Numerical modeling of yielding chain pillars in longwall mines

Salah Badr, Andrew Schissler, Miklos Salamon & Ugur Ozbay

Department of Mining Engineering, Colorado School of Mines, Golden, Colorado, USA

ABSTRACT: The practice in thick seam long wall mining at depths of 500 m and more shows that considerable sloughing of chain pillars, sometimes accompanied by bumps, may occur during development stage. The ability of these pillars to continue functioning as roof support during development and longwalling stages has to be assured for a safe and economical mining operation. Although already being used, little is known quantitatively about the response of these "yielding" chain pillars to varying loading conditions that come about during different stages of longwall mining. The paper presents the results from case history reviews and numerical modeling studies performed with the objective of improving the understanding of yield pillar behavior. The case history review indicates that yield pillars with width:height ratios 3 to 6 performed satisfactorily. The numerical modeling studies using a three-dimensional finite difference code FLAC3D [1] allowed realistic simulations of complex mining geometries and loading conditions of longwall mining. The numerical model incorporates a strain-softening constitutive model for post-peak pillar behavior and a non-linearly elastic material behavior for simulating gob compaction. The differences in performance of pillars with strain softening material and traditional Mohr-Coulomb material are also highlighted.

1. INTRODUCTION

Yield pillars are used in a variety of situations in many types of underground mining. In spite of considerable research work and decades of experience accumulated in their application, there are still uncertainties regarding behavior and performance of yielding pillars.

In the case of deep longwall mines, the need for yield pillar use arises due both to safety and economical reasons. Current regulations in USA require minimum three entries in longwall gate roads. Using most commonly accepted pillar strength formulae, it can easily be shown that at depths of about 500 m or more the sizes for solid pillars become too large for both safety and economics. Large pillars can be potential sources for bumps and also may fracture the roof or floor causing roof failures or floor heaves. From economics point of view, large pillar development layout means increased coal volume being left behind and also slowed down development process due to increased crosscut lengths.

Too small solid pillars can also be dangerous. Below 500 m cover, the entry sidewalls would start failing even before the formation of pillars. As will be shown later, at a depth of 600 m, the extent of sidewall fracturing reaches as deep as two meters

into the ribs. When the pillars are formed between entries, their sides may have extensively failed. In case of these pillars completely losing their load bearing capacity, the entry width would effectively more than double and could cause roof failures.

A simple pillar strength calculation would show that small coal pillars under 500 m cover in a gate road development would have safety factors less than one, which suggests that these pillars are loaded close to or beyond their strength. The conditions of these pillars as chain pillars in deep longwall mines and their responses to various loading stages during longwalling are not well understood. Miners have been using these "yielding" pillars over many decades, however, forming them mostly on the basis of trial and error. Dangerous situations may be created during experimentations with yield pillars and it is desirable and useful for the mining industry to have rationally established design guidelines and methods for these pillars. The road to developing rational design methods has to go through a better understanding of the performance and behavior yield pillars and this is the main theme addressed in this paper.

The subject of yield pillar behavior has been investigated in the past mainly using analytical methods and field instrumentations. These investigations produced information on load-

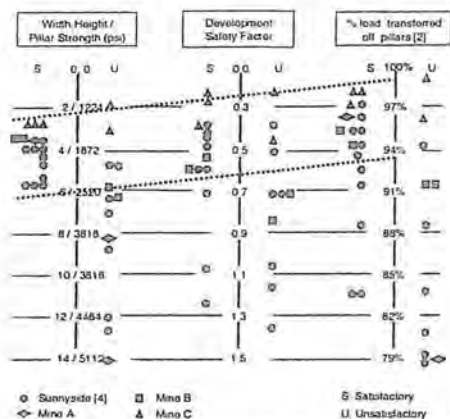


Fig. 1. Yield pillar performance categorized under common parameters used for pillar design.

bearing capacity, onset and development of fracturing in pillars and potential for unstable failures if pillars are incrementally load beyond their capacity. The studies mostly assumed 2D geometries and often made assumptions with regard to loading conditions during various mining stages and behavior of pillars in the post-peak regime. The influence of gob behavior on pillar loading is almost always ignored in the analytical studies. Current numerical models can deal with most of the difficulties encountered in analytical methods by allowing incorporation of 3D geometries and experimentations with non-linear materials such as strain softening for coal seam and compacting caved material in the gob area.

The paper starts with presenting the results from a review of yield pillar applications as practiced in four deep longwall mines. A 3D numerical model of longwall mining is then described and the results obtained from its use are presented. The strain-softening constitutive behavior and non-linearly elastic gob compaction models used for the modeling studies are discussed. The differences in modeling of yielding pillars between using strain softening and traditional Mohr-Coulomb plasticity models are also highlighted.

2. CURRENT PRACTICE

A review was carried out to determine the practices used for designing yielding pillars in deep coal mines. The cases chosen for review had documented histories of pillar performance and were instrumented using closure meters and borehole pressure cells installed in the pillars. Those operations had depth of cover ranging from

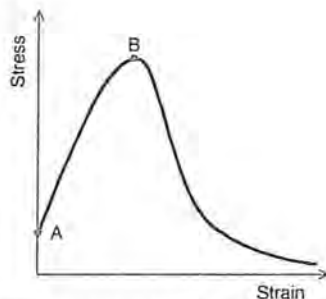


Fig. 2. Pillar complete stress-strain curve. A is vertical component of virgins stress B is pillar strength.

350 m to 900 m and mining height from 2 m to over 3 m.

Fig. 1 is a summary of the yield pillar design practices in four deep longwall mines [2]. The first criterion used is the width to height ratio. The data suggests a grouping of successful case histories within a range of three to five. The second criterion is development load stability factor in which the natural group of successful cases ranges from 0.4 to 0.6. The final group is using the quantity of load shed of the pillar using the Carr-Wilson [3] approach. This data suggests a successful grouping from 93% to 98% shed load.

The dotted lines in Fig. 1 highlights these ranges. The criteria for successful versus unsuccessful cases are that the descriptions of successful cases had no mention floor heave, bumps, bursts or roof problems. Unsuccessful instances are those where floor heave, bumps, bursts or roof problems are mentioned in the case history.

3. BASIC PRINCIPLES

3.1. Yield Pillar Principles

The earlier discussion suggests that many benefits would arise if the size of chain pillars were made with small width:height ratios. However, the strength of small pillars is insufficient to support the tributary load. How could these small pillars provide in these circumstances adequate roof control? The discovery that the stress-strain curve of rocks (Fig. 2), in addition to its well known ascending part (between points A and B), also has a descending part (beyond point B) [5,6], has led to an understanding of some counterintuitive ideas. This fundamental advance has led to the realization that the load-deformation curve of rock pillars is similar to that shown in Fig. 2; it also has an ascending and a descending branch [7]. When the state of a pillar is in the descending, or strain

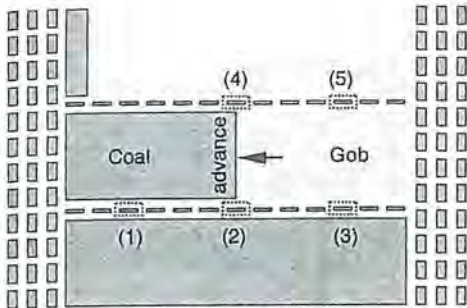


Fig. 3. Five stages loading of yield pillars.

softening part of the curve, the pillar can be termed as a yielding or "yield" pillar. Thus, the curve in Fig. 2 could also represent the deformation of a pillar. This is perhaps the simplest and most logical definition of yield pillars.

A chain pillar becomes a yield pillar as a result of progressive loading. Due to extraction of coal in the vicinity, the pillar load, or the average vertical stress acting on the pillar, gradually increases from the initial virgin value towards the pillar strength. In this phase of loading, both the pillar load and the mean pillar deformation, or compaction, are increasing simultaneously, that is, the pillar is in the ascending branch of the deformation curve, Fig. 2. The pillar load corresponding to the peak (point B) of the curve is the maximum load bearing capacity or the strength of the pillar. If the pillar deforms beyond point B, that is, the pillar is yielding, it can still sustain load but its load bearing capacity diminishes with increasing deformation. This property of yielding pillars has an important consequence.

A pillar can only be loaded beyond its strength if it can shed load, that is, some part of the pillar load can be transferred to another load bearing area. Load shedding can take place if three criteria are satisfied: a) there are load bearing areas (unmined seam or compacting gob) nearby which can sustain the transferred load, b) the roof and floor are sufficiently competent to facilitate the load transfer without debilitating roof fall or floor heave, and c) the stiffness of the surrounding rock mass is sufficiently high to ensure that the equilibrium of the rocks remain stable. If one or more of these criteria are not satisfied, the pillar will collapse and this collapse may be sudden or uncontrolled. The conditions that determine whether the pillar failure is sudden or gradual are not discussed here but have been defined elsewhere [7].

3.2. Loading of Chain Pillars during Retreat Longwalling

In Fig. 3 a plan view of a longwalling system, using two entries for development are depicted. Three longwall panels are shown, the upper one is already extracted, the panel at the bottom of the illustration has been developed, but the coal extraction has not commenced yet. As the longwall face in the middle panel moves from right to left as indicated, the chain pillars undergo five stages of loading. These stages are indicated in the diagram; the first three are shown to affect the pillars next to the head gate and the last two relate to the tailgate.

Stage 1 corresponds to the situation where the pillars are loaded only as a result of the virgin stresses and the stresses induced by the development of the entries and crosscuts in the vicinity. Stage 2 refers to the situation where the front abutment of the approaching face contributes to the loading. In Stage 3 the development is affected by the gob on one side and a still unmined ribside on the other side. The gob in the vicinity of the development is not fully compacted so it does not support the full weight of the overburden. Hence, the chain pillars and/or the ribside must support a portion of the load that corresponds to the full weight of the undermined overburden in the panel.

On the tailgate side, pillars situated considerably ahead of the face are subjected to the loading conditions corresponding to Stage 3. Now in Stage 4, as the face approaches, the front abutment increasingly contributes to the loading, hence the environment around pillars become progressively more adverse. Stage 5 corresponds to the situation where the influence of the face is no longer detectable and the chain pillars are surrounded on both sides by gob only. Thus, only the pillars themselves prevent the uniform settlement of the roof mass. From the pillars point of view, this situation is likely to be the most unfavorable.

In a relatively recent application of this mining technique the chain pillars, at a depth of 700 m, were approximately 8 m wide, 26 m long and 3 m in height. Quick calculations, based on the assumption of tributary loading, indicate that both the linear and power formulae yield a safety factor of 0.23. The probability of survival at this safety factor is negligibly small [8]. This result suggests that if chain pillars of this size were to be formed in a longwall layout at 700 m depth the pillars, if they would survive at all, would already be yield pillars in Stage 1. Thus, the success of retreat longwall mining at great depths depend on whether it is

possible to mine through all or, at least, three or four stages of mining with yield chain pillars. The answer to this question is not obvious. Pillar failure or bump, or debilitating deterioration of entries could hinder or even prevent successful mining operations.

Closer examination of the loading stages suggests that the transitions from Stage 2 to 3 and then into Stage 4 are the most critical periods of the operation. In Stages 1 and 2 it is relatively easy to visualize that the two entries and the pillars can be kept in order with relatively minor secondary support. However, when the face passes a pillar then at one side of that pillar a very wide cavity appears. Now the possibility emerges that the edge of the gob will override the chain pillars and moves up against the solid ribside. In this situation the chain pillars play a role very similar to that of the face support. Thus, the success of the method depends on whether the yield pillars at this stage can fulfill a role analogous to that of the face support and can protect the entry next to the ribside from the encroachment of the gob. It might be argued that the pillars can fulfill this role, provided their load bearing capacity at this stage is comparable or higher than that of a successful face support. In Stage 5 the principles do not change, but the conditions become more adverse. However, at this stage the entry, unless it is required for ventilation purposes, can be abandoned and the pillars can collapse, provided they do this in a gradual or controlled fashion.

4. RESEARCH NEEDS

The scenario outlined in the previous sections involves a number of difficult problems in rock mechanics. This does not mean to imply that such longwall operation are not planned and implemented. Several case histories of retreat longwalling with yield pillars at depth have been documented [2,3,4] and these descriptions indicate that previous designs enjoyed mixed success.

Since the whole idea of yield pillars hinges on the notion of strain softening, it is clear that the design method must incorporate the strain softening principles. Software development for a strain softening material is a difficult task, because the problem is non-linear and, even more importantly, the problems set in this type of substance are only conditionally stable. The only well developed software that can handle such laws is the well-known FLAC [1] package marketed by Itasca.

The geometry of chain pillars does not lend itself to two-dimensional treatment. This is so because the

behavior of pillars is likely to be influenced not only by its smaller width but also by its length and by the interaction between the pillars, the longwall face and the presence or otherwise of crosscuts. For these reasons the decision was made to work both with the 2D and 3D versions of FLAC. Unfortunately, due to the complexity of the mining geometry and of the constitutive laws, the progressive nature of mining that creates the five stages of loading, the numerical solution of problems in FLAC, especially in its 3D version, are cumbersome and time consuming. Thus, to make reasonable progress, a number of compromises had to be accepted in the models used.

An interesting feature of longwall mining is that as the coal in the panel is extracted, the upper strata will subside and settle on the gob, that is, on the fractured, particulate material that is created by the caving process. As a result of this subsidence the gob (particulate material) is compacted and gradually accepts a greater and greater load. This process relieves the chain pillars of some of their burden. This is essentially a statically indeterminate problem that cannot be solved without considering the deformation of the gob and the surrounding strata. As this is an essential aspect of the problem a great deal of effort was devoted to the correct modeling of gob behavior. This work was based on an adoption of the principles presented some years ago [9].

5. NUMERICAL MODELING

The numerical modeling studies were carried out using the commercially available FLAC3D [1] finite difference code. Detailed modeling of entry development and subsequent longwall retreat mining are incorporated into the model to account for the five stages of pillar loading shown in Fig. 3.

5.1. Strain softening coal material

The coal seam and pillars are modeled as strain softening material. The material properties of the strain softening material are (the same as the 2D FLAC model reported in [10]): in situ coal cubic strength, $K = 6.2$ MPa, friction angle = 30° , post-peak slope = -1.0 GPa/strain and residual cohesion = 0.05 MPa. Additional simulations were also carried out with coal being modeled as traditional Mohr-Coulomb material.

5.2. Gob simulation

The gob behavior is based on the "compaction" model [9]. Vertical stress σ_v in the gob increases exponentially with increasing vertical strain ϵ_v according to the formula

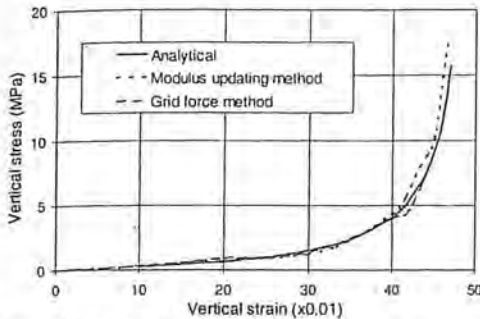


Fig. 4. Comparison of gob models.

$$\sigma_v = \frac{a\varepsilon_v}{b - \varepsilon_v} \quad [\text{Eq. 1}]$$

where a is a constant determining gob's deformation modulus and b is the limiting vertical strain. Based on the studies carried out at USBM [11] on gob behavior, the values for the constants were taken as $a=3.5$ MPa and $b=0.5$.

Two different algorithms are considered for implementation of the gob behavior of Eq.1 in FLAC3D model. In the first method, the compaction load is modeled as a sum of the vertical forces applied at the grid points of roof elements behind the longwall face. After a mining step, vertical strain in a particular zone in the gob area is retrieved and used to calculate the vertical stress according to Eq. 1. Grid reaction forces could then be calculated by multiplying vertical stress by the corresponding roof element's area. This model will be called "grid force" method. In the second method the gob is modeled as a non-linear elastic material. Its elastic modulus is continually increased as function of vertical strain_v induced in the gob area [12]. The algorithm for this "modulus updating" method uses bulk modulus K for each zone calculated from

$$K = \frac{1.75}{0.5 - \varepsilon_z} \quad [\text{Eq. 2}]$$

where ε_z is the vertical strain in the zone.

The gob compaction curves of two different algorithms as implemented in FLAC3D are compared in Fig. 4. As shown, both algorithms compare well with the analytical model. Since the grid force algorithm required long run times and laborious calculations, the modulus updating method was accepted as the standard gob model for FLAC3D longwall simulations.

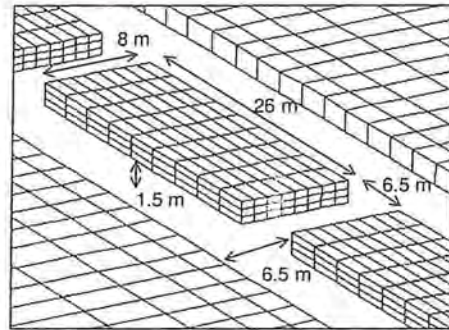
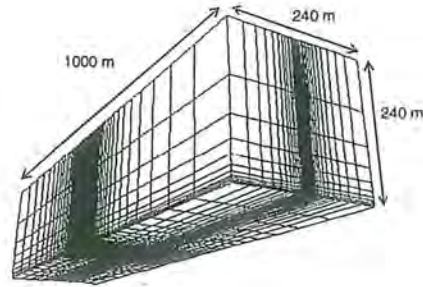


Fig. 5. FLAC3D grids. Top: Full block; bottom: entries and chain pillars.

5.3. Model Parameters

The FLAC3D longwall model has the same material and geometrical parameters of the previous 2D FLAC model [10] for comparison and continuation purposes. As was the case in the 2D model, the current model represents a two-entry system, with 3 m mining height longwall mine at a depth of 700 m. Pillars are 8 m wide and 26 m long separated by 6.5 m wide entries and crosscuts. A 3D block view of the model is shown in the top diagram of Fig. 5. To improve the accuracy of the analyses, the grid density at the model's center increases to give eight equal sized grids across the pillar width (Fig. 5-bottom). Most of the modeling results on pillar performance reported in this paper are obtained along a "scanline" placed across one of the pillars in

Table 1. Material properties used for FLAC3D simulations.

Property	Value
Horizontal / vertical stress	1
Virgin stress	17 MPa
Coal elastic modulus	3 GPa
Roof and floor elastic modulus	20 GPa
Poisson's ratio	0.25
Interface cohesion	0.5 MPa
Interface friction angle	20°

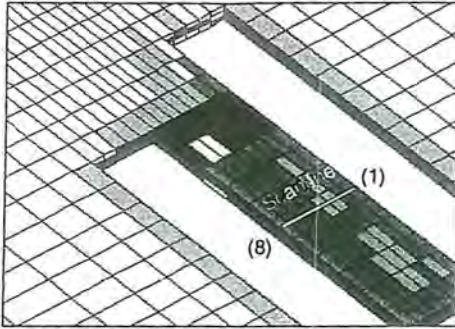


Fig. 6. Flac grid showing the entry development and scanline position after the entry faces passed it. Shading refers to various degrees of failure. The numbers are the start and end of the pillar grids shown in Fig. 7.

the central area as shown in Fig. 6. Material properties used are given in Table 1.

5.4. Modeling of pillars and entry development

The model first develops the gate road entries. The face advance rate is 3 m per mining step in the denser grid area at the center. Fig. 6 shows a particular geometry of the right entry leading the left one by 9m. As also seen, within the front and sides of both faces, there is a "process zone" of high stress and failed regions. The extent of this zone depends on the lead - lag distances of the advancing faces and other geometrical parameters. The development faces and sidewalls are all in a failed state when they are exposed.

Details of the failure in the process zone and chain pillars are further illustrated in Fig. 7, which shows the history records of the stress-strain relationships for eight zones along the scanline. Zone 1 starts failing before the face of the leading entry approaches the scanline. Zone 1 fails completely as soon as it is exposed and its failure triggers failure of Zone 2. At this stage, the development face is next to the scanline. Zones 3 and 4 fail as the entry face passes the scanline, but less drastically than the failures in Zones 1 and 2 due to higher confinement at their locations. Failed region extends to Zone 5, which has a shallower post peak curve and higher residual strength than the first four. The last three zones are unfailed at this stage. As the second entry face approaches to the scanline, the stress in Zone 8 first increases and then drops, with a steepest slope compared to the failure slopes of the other zones. Zones 7 and 6 and finally 5 fail as second entry passes the scanline position. When the pillar is fully formed, all the zones are at their residual

strength. The central zones bear higher stresses than the side zones.

The solid line in Fig. 8 is a re-plot of Fig. 7 after averaging the stress-strain values of the eight zones. The dashed curve in this figure is the result from the 2D model in a previous study [10]. Both 2D and 3D models show a small stress increase at the beginning. This is due to averaging the stress over the scanline, which includes failed zones closer to the entry and higher stressed zones further into the coal seam. When fully formed, both pillars are at their residual strengths. The steeper post peak curve of 3D pillar is possibly due to the failure ahead of the entry face, which could not be modeled in 2D. The peak and residual strength values of 2D and 3D pillars are similar.

For comparison purposes, the 3D strain softening

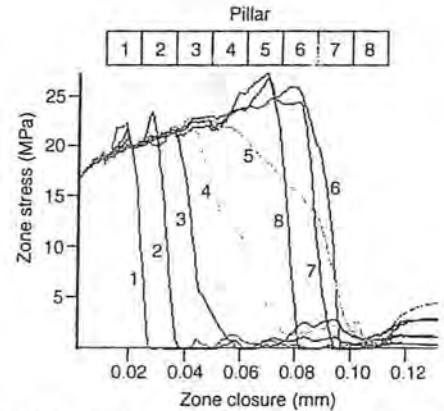


Fig. 7. Stress-strain curves across a yielding chain pillar (top - see also Fig. 6 for pillar grid positions along the scanline) as obtained from FLAC3D using strain softening.

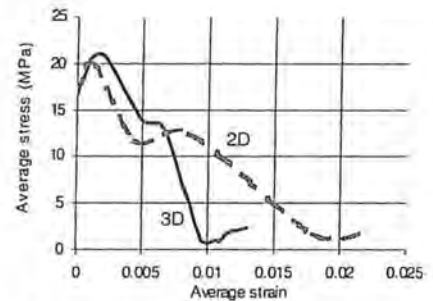


Fig. 8. Average stress-strain relationship of the yielding chain pillar modeled using 3D and 2D [10] FLAC codes.

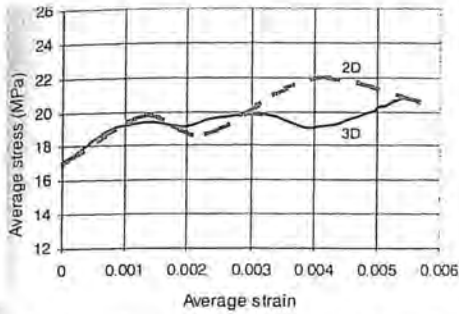


Fig. 9. Comparison of 2D and 3D pillar stress-strain curves obtained using traditional Mohr-Coulomb criterion.

simulations were repeated using traditional Mohr-Coulomb plasticity for the coal seam. Fig. 9 shows the results. For both cases, the stresses in the fully formed pillars are much higher than the strength estimates of most common empirical pillar strength formulae. In Fig. 10, the stress histories of 3D chain pillar modeled as strain softening and Mohr-Coulomb materials are plotted. The strain softening pillar has a steep stress drop while the Mohr-Coulomb pillar hardens. It is believed that the strength parameters used for strain softening material and Mohr Coulomb material are the lower and upper bound parameters. Further back analysis studies are required to improve the model parameters for more realistic simulations.

5.5. Longwall mining and gob compaction:

The longwall face advances are introduced initially 150 m steps in the large grid area and then gradually reduce down to 3 m per mining step in the central part of the model. Fig. 11 shows the gob stress plots at a point in the first cut area. The first longwall produces about 15 percent closure in the

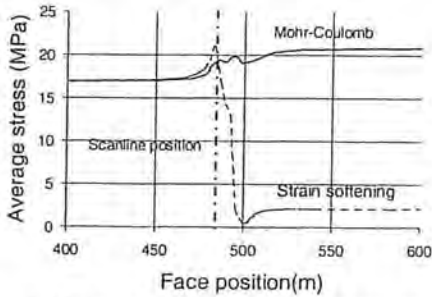


Fig. 10. 3D chain pillar modeled as strain softening and Mohr-Coulomb materials.

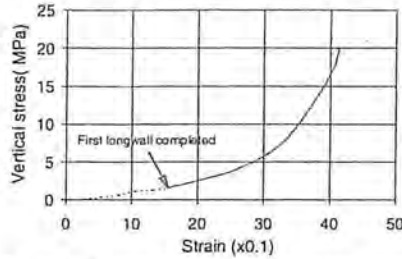


Fig. 11. Gob compaction curves after mining two panels.

back area. The second longwall produces a greater compaction than the first partly due to the merging of the effect of the two panels and partly due to the symmetry conditions imposed on the sides of the specimen. The overall behavior is an asymptotically increasing gob stress with increasing compaction, approaching virgin stress levels.

The stresses in chain pillars after they are formed during the development stage are observed as not being affected by the advances of longwalls. This is possibly due to the relatively low width:height ratio of pillars and/or treatment of residual strength in the strain softening model. The compression of pillars due to longwall mining is shown Fig. 12.

6. CONCLUSIONS

1. Yield pillars loading and behavior in the post peak regime involve complex mechanisms and need to be analyzed in three dimensions using appropriate constitutive laws.
2. Initial results from case history studies indicate that pillars with width:height of 3 to 5 have been more successful as yield pillars than the others
3. Gob compaction and strain softening

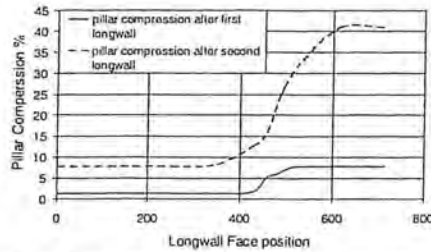


Fig. 12. Pillar compression recorded along the scanline position

models adopted for the FLAC3D simulations gave reasonably realistic behavior of pillars and gob area. Of the two gob compaction algorithms used for the simulations, the modulus updating method proved to be more practical than the nodal force method

4. It is believed that the strength parameters used for strain softening material and Mohr-Coulomb material are the lower and upper bound of the strength parameters used for the coal seam. Among the strength parameters, the negative slope and friction angle play a major role in quantification of the results. More work is required to quantify the numerical values of these parameters.
5. The flat response of strain softening pillars to further compaction at residual strength level needs to be further investigated.
6. It is noteworthy that, due to the complex geometry, the computation involved in a 3D solution still represents a demanding task in spite of the recent growth in computing power.

7. ACKNOWLEDGMENT

This publication was supported by Cooperative Agreement number U60/CCU816929-02 from the Department of Health and Human Services, Center for Disease Control and Prevention (CDC). Its contents are solely the responsibility of the authors and do not necessarily represent the official views of the Department of Health and Human Services, CDC. Support provided by Department of Health and Human Services, CDC, is greatly acknowledged. The work presented is part of the Health and Safety research activities currently carried out at Western Mining Resource Center (WMRC) at the Colorado School of Mines.

We also gratefully acknowledge Drs. Peter Cundall and Pedro Varona from HCITASCA for their advice on gob modeling.

REFERENCES

1. FLAC3D 2002. Itasca Inc. Minnesota.
2. Schissler, A. (2002) Yield pillar design in non-homogenous and isotropic stress fields for soft minerals. Ph.D. Thesis in preparation. Department of Mining Engineering, Colorado School of Mines, Golden, Colorado.
3. Carr, F. and A.H. Wilson (1982). "A new approach to the design of multi-entry developments for retreat longwall mining." Proc. 2nd Conf. On Ground Control

in Mining, Ed.: S.S. Peng. West Virginia University, Morgantown

4. Koehler, J. R. (1994) History of gate road performance at the Sunnyside mines: Summary of U.S. Bureau of Mines Field Notes. IC/9393.
5. Cook, N.G.W. (1965) "The failure of rock." Int. J. Rock Mech. Min. Sci. v. 2, 389-403.
6. Deist, F. (1965) "A non-linear continuum approach to the problem of fracture zones and rockbursts." J. S. Afr. Inst. Min. Metall., v. 65, 502-522.
7. Salamon, M.D.G. (1970) "Stability, instability and design of pillar workings." Int. J. Rock Mech. Min. Sci. v. 7, 613-631.
8. Salamon, M.D.G. (1999). "Strength of coal pillars from back-calculation." Proc. of the 37th U.S. Rock Mechanics Symposium. Vol. 1, 29-36. Ed.: B. Amadei, R.L. Kranz, G.A. Scott and P.H. Smeallie. A.A. Balkema, Rotterdam.
9. Salamon, M.D.G. (1991) "Displacements and stresses induced by longwall mining in coal." Proc. 7th Congr. of the Int. Soc. for Rock Mech., Aachen. Ed.: W. Wittke, 1199-1202. Balkema, Rotterdam.
10. Ozboy, U, Salamon, M. D. G. and Lee, K. K. 2001. Rational design of yield pillars: Improved understanding of yielding mechanism. *SME Annual Meeting*. Denver, Colorado. February 26-28, 2001
11. Deno M. Pappas and Christopher Mark 1993 (Behavior of Simulated Longwall Gob material) United States Department of the Interior- Bureau of mines- Report of investigation No. 9458.
12. Cundall, P. 2001. Personal correspondence.

PROCEEDINGS OF THE 5TH NORTH AMERICAN ROCK MECHANICS SYMPOSIUM AND THE 17TH
TUNNELLING ASSOCIATION OF CANADA CONFERENCE: NARMS-TAC 2002
TORONTO/ONTARIO/CANADA/7 – 10 JULY 2002

NARMS-TAC 2002

“Mining and Tunnelling Innovation and Opportunity”

Edited by

Dr. Reginald Hammah

*Lassonde Institute, University of Toronto, Toronto, Ontario, Canada
Rockscience Inc., Toronto, Ontario, Canada*

Dr. Will Bawden

Lassonde Institute, University of Toronto, Toronto, Ontario, Canada

Dr. John Curran

Lassonde Institute, University of Toronto, Toronto, Ontario, Canada

Mark Telesnicki

Golder Associates Ltd., Mississauga, Ontario, Canada

VOLUME 1

University of Toronto/2002

Printed and bound by UNIVERSITY OF TORONTO PRESS, Toronto